Proposed Title:

Machine Learning-based Identification and Characterization of High-risk Carriers of HTLV-1-Associated Myelopathy (HAM)

Md Ishtiak Rashid[1], Junya Sunagawa[1], Akari Matsuki[2,3], Asami Yamada[4], Toshiki Watanabe[6], Masako Iwanaga[7,8], Ki-Ryang Koh[9], Takafumi Shichijo[4], Masao Matsuoka[4,5], Jun-ichirou Yasunaga[4*], Shinji Nakaoka[3*]

[1]Graduate School of Life Science, Hokkaido University, Sapporo, Japan.
[2]Quantitative Life Sciences, The Abdus Salam International Centre for Theoretical Physics (ICTP), Italy.
[3]Faculty of Advanced Life Science, Hokkaido University, Sapporo, Japan.
[4]Department of Hematology, Rheumatology, and Infectious Diseases, Graduate School of Medical Sciences, Faculty of Life Sciences, Kumamoto University, Kumamoto, Japan.
[5]Kumamoto Rosai Hospital, 1670 Takehararamachi, Yatsushiro, Kumamoto, Japan.
[6]Department of Hematology & Oncology, St. Marianna University School of Medicine, Kanagawa, Japan.
[7]Department of Clinical Epidemiology, Nagasaki University Graduate School of Biomedical Sciences, Nagasaki, Japan.
[8]Nagasaki Genbaku Hospital, Nagasaki, Japan.
[9]Department of Hematology, Osaka General Hospital of West Japan Railway Company, Osaka, Japan.

Abstract

HTLV-1-associated myelopathy (HAM) develops in a part of HTLV-1-infected individuals while most of the individuals remain asymptomatic. This complicates the identification of HTLV-1 carriers at elevated risk. In this study, we integrated HTLV-1 proviral load and antibody titers against Tax, Env, Gag p15, p19, and p24 proteins in a machine learning (ML) framework to identify and characterize high-risk individuals likely to develop HAM. We stratified asymptomatic carrier samples employing an anomaly detection model. We further developed and validated classifier models capable of distinguishing three clinical subgroups, carrier, ATL, and HAM for assessing the anomaly carrier samples as unseen test data. With most anomaly carrier samples (~76.47%) predicted as HAM, further statistical and interpretative analysis revealed the 'HAM-like' characteristics of the anomaly carrier samples indicating elevated risk. Additionally, significant heterogeneity in immune response was observed among other asymptomatic carriers. Our machine learning-based approach offers a novel and insightful tool for identifying and evaluating high-risk characteristics for HAM, providing a holistic view of the complex immune dynamics of asymptomatic carriers of HTLV-1.

Introduction

Human T-cell leukemia virus type 1 (HTLV-1) is the first identified retrovirus known to cause chronic lifelong infections in humans [1]. Following infection, it causes adult T-cell leukemia-lymphoma (ATL), a form of blood cancer, and HTLV-1-associated myelopathy (HAM), a chronic inflammatory disease of the central nervous system. While most infected individuals remain asymptomatic, approximately 2 to 5% of HTLV-1 carriers develop ATL [2], and 0.25 to 4% develop HAM/TSP [3]. The annual national incidence rate of new HTLV-1 infections in Japan has been reported as 3.8 cases per 100,000 person-years [4]. The combined strategies of immune evasion and suppression allow HTLV-1 to remain in the host for a prolonged time without expressing symptoms which complicates the identification of carriers at higher risk of developing ATL or HAM [5][6][7]. ATL has been reported to occur in adults at least 20 to 30 years after the infection [8] and for HAM, the latent period ranged from 4 months to 30 years [9]. While it remains unknown why some HTLV-1 carriers develop the disease, it is of interest to develop methods that can identify high-risk asymptomatic individuals.

For HTLV-1-infected individuals, the diversity of the infected cells and immune responses is influenced by the interaction between the virus and the host's immune system. A disruption of the equilibrium between viral persistence and host immunity can trigger the onset of associated diseases. Distinct immunological responses may arise from impaired immune regulation against the HTLV-1 infection [10]. As reported previously, HTLV-1 infection evokes both cellular and humoral immunity [11][12][13]. Therefore, immunological markers can be instrumental in evaluating the risk of associated diseases. Although proviral load (PVL) has been considered a risk factor, its interpretation in asymptomatic carriers is still challenging due to individual variations and lack of definitive thresholds for disease risk [14][15]. Additionally, some studies reported the PVL quantity remains constant over several years, regardless of clinical manifestation [15][16][17][18]. However, antibody profiling, when combined with other markers like PVL, has been reported as useful for distinguishing asymptomatic carriers from ATL or HAM patients [19][20][21][22] and potential for predicting disease progression. Moreover, serum-based testing is simpler and cheaper than genetic analysis. Hence, analyzing antibody responses can provide a quantitative and specific method for identifying the infected individuals at elevated risk.

In our previous study using a modified Luciferase immunoprecipitation system (LIPS) assay, we screened patients for antibodies against each of the viral proteins, HTLV-1 Gag proteins (p15, p19, p24), Env, and Tax. Along with multivariate analysis of the antibody titers followed by targeted sequencing, we identified carriers at high risk for ATL. We also listed important factors for separating the HAM subgroup [21]; however, this finding might overlook the possibility that some carriers are already showing similar antibody responses to HAM/TSP and thus need to be explored in more depth. Although longitudinal studies are invaluable for observing the disease progression over time, it is still challenging given a prolonged latency period. Moreover, considering the treatment effects, it may not fully capture the hidden patterns within the data. Cohort studies usually maintain high data quality and standardized data collection protocols. This reduces noise and inconsistencies, making ML models more compatible and generalizable [23]. Machine learning (ML) models surpass the traditional

multivariate statistical methods by handling complex, high-dimensional data and uncovering non-linear patterns. Based on clinical data alone ML models offer a robust alternative tool within data-rich contexts [24][25][26][27].

In the present study, we developed a two-tiered ML-based framework integrating antibody titers to HTLV-1 PVL and Tax, Env, along with the immunogenic mature Gag p15, p19, and p24 proteins to identify and characterize the asymptomatic carriers with a higher likelihood of developing HAM. Collectively our results show that the ML-based approach can be effective in risk prediction and early intervention of HAM that might otherwise remain undetected through conventional diagnostic approaches.

Results

Detection of Potentially High-Risk Carriers

At the data preprocessing step, before applying ML models to our dataset, we handled the multicollinearity issue [28] by excluding Gag p19, based on the highest VIF score (see **Determination of Key Variables** in **Method** and Supplementary Table S1A and B for details). Out of 264 asymptomatic carriers, the Isolation forest model detected 17 carrier samples as anomalies, which we labeled as anomaly carriers (AC). One carrier who later developed HAM/TSP (CDH) was also identified as an anomaly and included in the AC group, suggesting that the Isolation forest model effectively filters carrier samples with a possible risk of HTLV-1-associated diseases. For details about the algorithm of Isolation forest and choice of hyperparameters, please see **Anomaly Detection by Isolation Forest Algorithm** in **Methods.**

Next, we compared the performance of four ML models based on PRAUC scores to classify samples into 3 subgroups: non-anomaly carrier, HAM/TSP, and ATL. We chose the Random forest model (RF) for its superior performance (See **Classification Modeling** in **Method** for details) [Supplementary Table S3]. The RF classifier model was used to predict the holdout set of AC samples (n=17). Interestingly, the classifier predicted the majority of AC samples (n=13 out of 17) as HAM/TSP [Figure 1]. The one CDH sample was also predicted as HAM/TSP by the classifier model. Moreover, in the case of 17 anomaly carrier samples, all the feature values showed a stronger positive correlation with their predicted probabilities of HAM/TSP except PVL [Supplementary Table S4].

Results of Partial Least Squares (PLS) distribution of sample groups further revealed that AC samples were localized near the HAM/TSP cluster [Figure 2]. This result combined with the classification result where most AC samples predicted as HAM/TSP, suggests that AC samples share significant similarities with HAM/TSP samples, further supporting our hypothesis that AC samples exhibit 'HAM-like' characteristics.

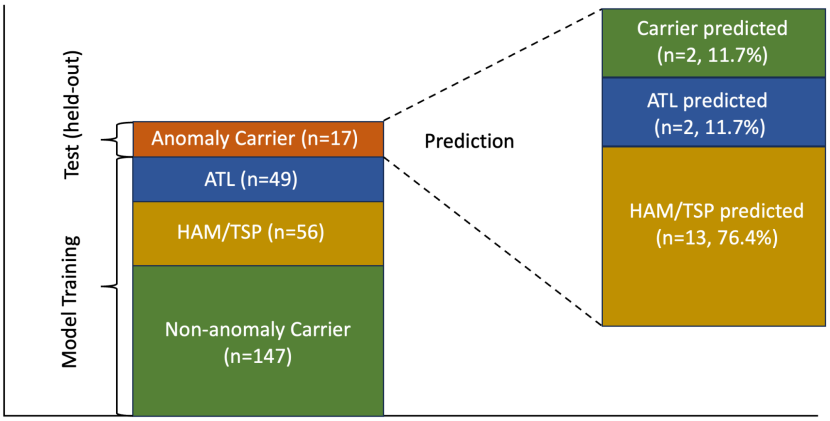

Figure 1: Illustration of the prediction results of anomaly carrier samples by the random forest classifier model. The left bar shows the training and test data for the classifier model. The model was trained on three sample groups and predicted the anomaly carrier samples as unseen test data. The anomaly carrier samples (n=17) were classified into three prediction groups:

Around 76.4% of the anomaly carrier data were predicted as HAM/TSP, whereas only 11.7% and 11.7% of the samples were predicted as ATL and carrier respectively (shown on the right bar).

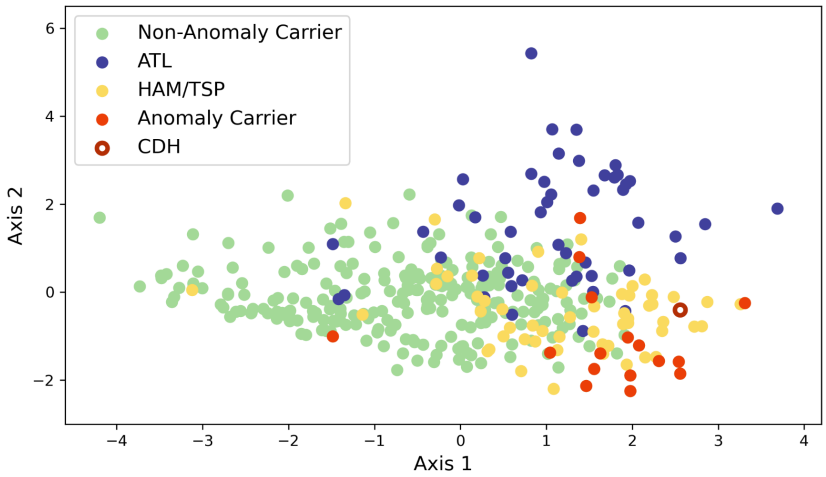

Figure 2: The PLS plane shows the distribution of all 369 samples from non-anomaly carriers (green), ATL patients (blue), HAM/TSP patients (yellow), anomaly carriers (red), and CDH (dark red as edge color and white-centered). Each dot on the plot represents an individual sample. This plot depicts the clustering of the sample groups based on the analyzed variables, where anomaly carrier samples were positioned near the HAM/TSP cluster.

Comparison of Feature Value Distributions among the Subgroups

Figure 3 compares the feature values of 4 subgroups. Between AC and non-anomaly carrier comparison, all features in the anomaly carrier were significantly higher. On the contrary, we found no statistically significant difference between AC and HAM/TSP for PVL ($p = 1.0$), Tax ($p = 1.0$), Gag p15 ($p = 0.34$), Gag p19 ($p=0.65$) and Gag p24 ($p = 0.89$) except Env ($p=0.0048$) (for details about the statistical tests, please see **Boxplot Visualization and Statistical Tests** in **Methods)**. These observations collectively indicate that AC samples display a high degree of similarity with HAM/TSP. Consistent with previous research [10], we found antibody responses to the immunodominant proteins (Env, Tax, Gags) higher in HAM/TSP patients (n=56). Conversely, PVL in ATL patients was significantly higher than in all other subgroups [Figure 3, Supplementary Table S6], which is consistent with previous studies [4][29][30].

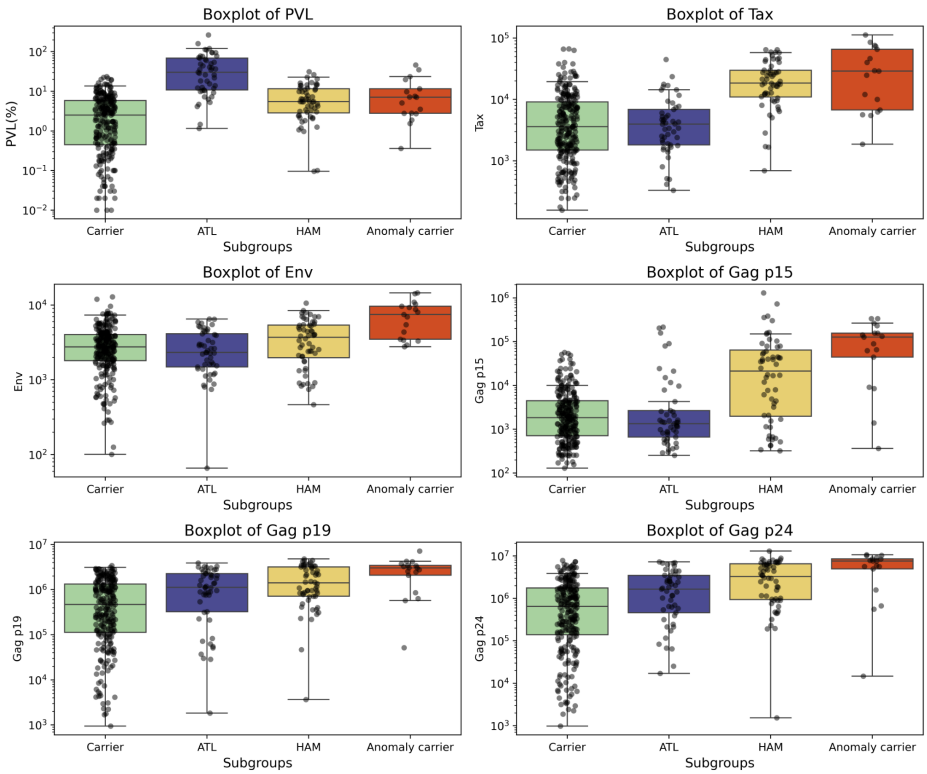

Figure 3: The boxplots collectively illustrate the distribution of PVL and Antibody titers to HTLV-1 antigens Tax, Env, Gag p15, Gag p19, and Gag p24 across different clinical subgroups: non-anomaly carrier (green), ATL (blue), HAM/TSP (yellow), and anomaly carrier (red). The individual data points overlaid on the boxplots show the actual distribution and density of the data.

Exploring Biomarkers for Anomaly Carrier Detection

To determine the crucial factors that characterize the anomaly carrier and HAM/TSP, SHapley Additive exPlanations (SHAP) analysis was performed. SHAP analysis is an interpretable machine learning framework that can assess the impact of each feature on the classification of each class (non-anomaly carriers, ATL, HAM/TSP, and anomaly carriers). Figure 4 shows the SHAP bar plot from the ETC classifier which performed the best [Supplementary Figure S6]. We found Tax is the most important feature for HAM/TSP, and Gag p24 for anomaly carriers, followed by Gag p15 and Env. Although the prediction above indicated high similarity between anomaly carriers and HAM/TSP subgroups, the ranking of feature importance differs qualitatively. Gag p15 and Env are influential features in anomaly carriers but their relative rankings are not uniformly elevated in HAM/TSP. Also, Tax exhibits a lower ranking in the anomaly carrier.

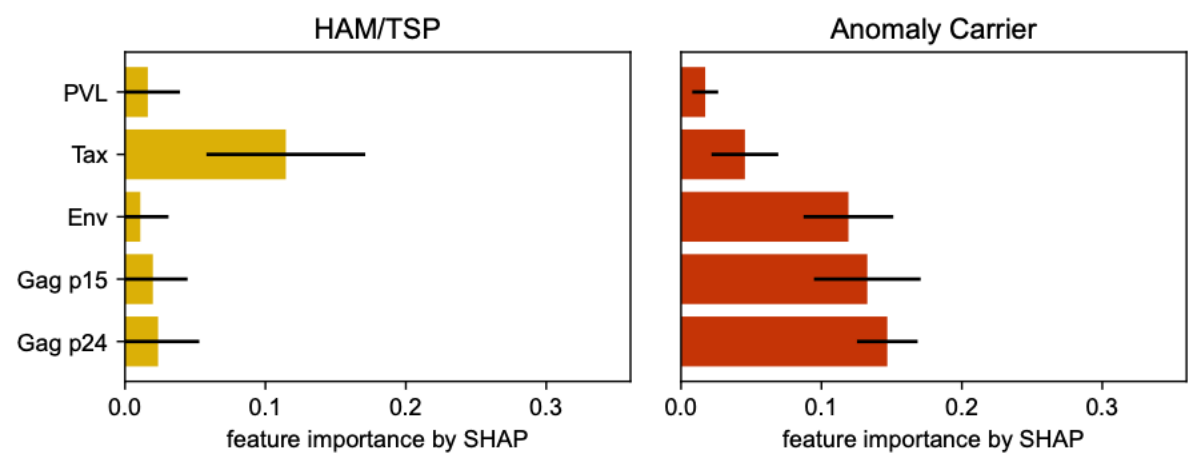

Figure 4: SHAP feature analysis of HAM/TSP and anomaly carriers. Each bar shows an absolute median value of 1000 iterations for different random seeds and the black line represents standard deviation. SHAP analysis for non-anomaly carriers and ATL is in Supplementary Figure S7.

Discussion

In this study, we developed a machine learning-based approach to capture HTLV-1 carriers at elevated risk of HAM progression. The Isolation forest anomaly detection algorithm identified a subgroup of anomaly samples from the asymptomatic HTLV-1 carrier population. Further characterization through classifier prediction and statistical analysis revealed that the anomaly carrier samples closely resemble the characteristics of HAM, suggesting a similar disease trajectory. Additionally, different patterns of antibody response were observed among the asymptomatic carriers and other clinical subgroups which enabled us to further investigate the risk factors. Finally, we utilized SHAP for comparative feature analysis among the sample groups (non-anomaly carrier, anomaly carrier, ATL, and HAM) to identify the key driving features that characterize each subgroup and contribute to the disease progression.

The main aim of this study was to shed light on asymptomatic carriers who are at a high risk of progressing HAM onset. With most of the anomaly carrier samples being predicted as HAM by the RF classifier [Figure 1], our hypothesis was further supported when the purposely included CDH sample in the carrier population was also identified as an anomaly and subsequently predicted as HAM. The potential similarities in the underlying profiles of the anomaly carrier samples are also reflected in their clustering near the HAM samples [Figure 2]. All features were significantly higher in anomaly carriers compared to non-anomaly carriers [Figure 3]. Elevated antibody responses in anomaly carriers might reflect the immune response have higher activity during disease progression. Interestingly, we found that only anti-Env antibody titer in anomaly carriers differed significantly from those of HAM [Figure 3, Supplementary Table S6], whereas other features showed no significant differences. Env is one

of the structural proteins of a virion and is necessary for cell-to-cell transmission. Thus it is a primary target of the antibody response [31, 32, 33, 34]. Furthermore, elevated anti-Env antibody responses have been associated with HAM patients in several studies, which supports our result [10, 19, 35, 36]. A novel implication is that, before onset, the rate of progression accelerates, as evidenced by the increased antibody levels. In HAM, the immune response is fully engaged; however, in progressive asymptomatic carriers, this saturation has yet to be achieved [19]. This phase might represent a snapshot of dynamic host-virus interaction where these rising antibody titers likely reflect the heightened viral activity and the immune system's escalating response as the disease advances toward clinical manifestation. Ultimately, a saturation point is reached at the onset of the disease, where antibody levels level off as the immune response shifts into a steady-state phase. This might be well reflected in feature analysis, where the SHAP value of Env is relatively high in the anomaly carrier, but not in HAM and non-anomaly carrier [Figure 4, Supplementary Figure S7].

We found Tax to be the predominant feature of HAM, consistent with findings from multiple studies. [19, 37]. Furthermore, prior studies have reported significantly higher antibody responses to Env and Gag proteins in HAM patients reinforcing their potential role in HAM patients [10, 19]. It is known that during infection, Gag and Env proteins are initially unpolarized in isolated T cells and accumulate at the cell-cell junction upon contact. Gag protein is subsequently transferred from HTLV-1-infected T cells to uninfected T cells [38]. Aligning with these previous observations, we interestingly found the feature values of Gag p15, p24, and Env of anomaly carrier samples exhibited a significant inverse relationship with their anomaly scores, i.e., higher feature values correspond to higher anomaly levels [Supplementary Table S2, Supplementary Figure S5][39]. Assessment of humoral immunity to Gag demonstrates potential as a biomarker for detecting high-risk individuals. In our study, we succeeded in suggesting that Gag p15 protein has some important function that may lead to developing HAM onset [Figure 3 and 4], however, we avoid attributing our result to some implications about Gag p15; further research is required to identify the specific function of these mature Gag proteins (p15, p19, and p24). It is noteworthy that, although the SHAP value of both Gag p15 and p24 falls within the high-ranking features that characterize anomaly carriers, we opted to exclude the interpretation of Gags (p15, p24) due to their inconsistent contribution patterns observed across the multiple classifiers employed in this study [Figure 4 and Supplementary Figure S7].

Identifying the risk for developing HAM onset is challenging compared to other HTLV-1-associated diseases. In the case of ATL, for example, the risk can often be characterized by the changes in the clonality of infected cells, since a single clonal infected cell expands during the viral progression. Also, several driver mutations are reported to stimulate malignancy, thus leading to the survival of pathogenic cells and outcompete other infected cells towards monoclonal proliferation [40]. While these promising markers can detect risks of ATL onset, HAM is less described for early diagnosis, due to the nature of its slow progression [41]. Moreover, complicated host immune responses against infected cells vary widely between patients with different lifestyles, which makes the prediction more difficult [42]. Having anti-Env at the top of the list, elevated antibody titer might be a key observation for evaluating

disease progression.

Of interest is the significant heterogeneity in immune response among the asymptomatic carriers in our study. Surprisingly, antibody responses (against Env, Tax, Gags, and PVL) in many asymptomatic carriers were observed at the same elevated level as that of HTLV 1-related diseases (ATL and HAM). This finding led us to our initial hypothesis to detect high-risk asymptomatic carriers (i.e., anomaly carriers) who are likely to progress to disease onset. Although heterogeneity seems to be obvious when considering the various lifestyle backgrounds of patients, it is noteworthy to confirm it based on our large number of asymptomatic carrier data.

Our work acknowledges some limitations. First, we don't have information on anomaly carriers whether they develop HTLV-1-related diseases or not in the future except for one sample who was diagnosed as HAM later on (CDH). To fully evaluate the prediction and the hypothesis of our result especially for HAM/TSP, further data accumulation would be critical (a prospective study like [14]). Second, little is known about the relationship between the antibody titers and the host immune defense as mentioned above. For the data from the LIPS assay to be used as a clinical diagnosis, these interplays should be explored in more depth. Furthermore, inconsistent results in antibody titers from previous studies have discouraged clinical application, which makes it difficult to choose consensus cutoff values for disease distinction [41]. While cross-validation offers robust internal validation, we acknowledge the necessity of an independent dataset for evaluating the model's generalizability. Future research should aim to include external validation cohorts to confirm our model's applicability.

Methods

Ethics statement

This study was performed in accordance with the Declaration of Helsinki and was approved by the Ethics Committees of Kumamoto University (accession numbers: G489, G499, and E2214). Written informed consent was waived because of the retrospective design. Consent for publication was obtained from all patients.

Study Population

The data used in this study was published previously by Yamada et al. [21]. PVL and antibody titer data (non-time series) were collected against HTLV-1 antigens Tax, Env, Gag p15, p19, and p24 using LIPS assay. Our previous study reported 24 carriers who later developed ATL (CDA) were considered as ATL in this study. We also had only one carrier who later developed HAM/TSP (CDH) and it was purposefully included in the carrier population. Therefore, we focused our study on 264 asymptomatic carriers, 49 ATL, and 56 HAM/TSP patients.

Determination of Key Variables

Initially, Spearman's rank correlation revealed a significant correlation between Gag p19 and p24 [Supplementary Figure S2]. To address the multicollinearity issue and choose the variables to use in the ML analysis, the Variance Inflation Factor (VIF) score was used [28]. See Supplementary Tables S1A and S1B.

Anomaly Detection by Isolation Forest Algorithm

For identifying potential outliers or anomalous data points from the asymptomatic carrier population (n=264), we applied the Isolation Forest algorithm, an unsupervised machine learning technique based on decision trees. For each datapoint (sample), the following process is repeated until the datapoint is isolated:

1. Randomly select a feature (e.g. PVL)
2. Randomly choose a threshold between the maximum and minimum values of the selected feature (e.g. PVL=0.1) and divide the data points below and above the threshold.

The key idea is that data points with anomalous feature values are likely to be isolated with only a few iterations. The algorithm constructs an ensemble of isolation trees for a given dataset and uses the path length from the root to the leaf to determine the anomaly score. Given m is the number of data points, the anomaly scores s for a datapoint x is defined as

$$s(x,m) = 2^{\frac{-E(h_i(x))}{c(m)}}, \qquad (1)$$

where $h_i(x)$ represents the path length for the i -th isolation tree, $E(h_i(x)) = \sum_i h_i(x)$ denotes the average path length across the ensemble of isolation trees,

$$c(m) = \begin{cases} 2H(m-1) - \frac{2(m-1)}{m} & (m > 2) \\ 1 & (m = 2) \\ 0 & (\text{otherwise}) \end{cases}$$

is the average path length for a dataset with m points, utilized as a normalization factor [43], and $H(k)$ is the harmonic number. The sklearn implementation of the decision function of Isolation Forest yields negative anomaly scores, where lower (negative) scores indicate potential anomalies [39].

By applying a cutoff threshold at -0.05 to the anomaly scores of the Isolation forest, we isolated the anomaly data points for further investigation [44]. This threshold was strategically chosen to capture approximately 5% of the most extreme anomalies (inversely corresponding to the 95th percentile of the normal data distribution) from our carrier population [Supplementary Figure S4]. Since around 4% of the carriers develop HAM/TSP [3, 45], we aimed to mirror this proportion.

The resulting anomaly carrier samples were then removed from the carrier data and considered as a holdout test set (unseen data) for further classification analysis. The remaining non-

anomaly carrier, ATL, and HAM/TSP samples were used for training and cross-validation of the classifier models. Additionally, the feature values of the anomaly carrier samples were tested for Spearman correlation analysis with their anomaly scores. The difference between the sample groups was evaluated by plotting all the samples in a PLS plane.

Classification Modeling

During data preprocessing, we randomly downsampled 100 carriers since the dataset was highly imbalanced. In this study, we employed the One-vs-Rest (OvR) approach to address the multiclass classification problem. This approach breaks down the multiclass classification into multiple binary classification tasks, where one classifier is trained for each class against all others. To determine the best-performing model, we evaluated four different classifiers: Random Forest classifier (RF), XGboost Classifier (XGB), Extra Trees Classifier models (ETC), and Support Vector Machine (SVM). Nested cross-validation (CV) was used to ensure robust performance evaluation and avoid overfitting. Particularly, an outer cross-validation loop was used to assess the model performances, while an inner loop was used to optimize the hyperparameters of each classifier using GridSearch.

In the inner loop, within each training set of the outer cross-validation, a 3-fold cross-validation was conducted for hyperparameter tuning and the combination that maximized the classifier performance based on the overall mean Area Under the Precision-Recall Curve (PRAUC) score was selected [46]. This ensured optimal parameter selection for each model. The model's generalization performance was evaluated in the outer loop using a 5-fold cross-validation. For each fold, the dataset was partitioned into training and validation sets. The optimal hyperparameters identified in the inner loop were applied to train the classifier on the training subset, and the model's performance was subsequently tested on the reserved test set. This process was repeated across all folds, and the average performance metrics were reported. Finally, the best classifier identified through nested CV was subsequently trained on the entire training dataset from the outer cross-validation and used to predict outcomes on the holdout test set (anomaly carrier samples). The predicted probability of HAM/TSP among the anomaly carrier samples (holdout test set) was calculated, followed by a correlation analysis of the predicted probabilities and their feature values. The workflow is depicted in [Supplementary Figure S1]. For the classification models performed in this study, the implementation available in the sklearn library was used [39]

Boxplot Visualization and Statistical Analysis

We employed a combination of visual and statistical methods facilitating an initial comparison of the feature distributions among different sample groups including anomaly carriers. The Kruskal-Wallis test was performed, with a significance level set at $\alpha = 0.05$. P-values were adjusted for multiple comparisons using the Bonferroni correction method for Dunn's post-hoc analysis to maintain the overall type 1 error rate. The statistical analysis was performed using the Python Scipy package [47, 48].

Interpretation with SHapley Additive exPlanations (SHAP) analysis

As an approach to interpreting the model's behavior, the Shapley Additive exPlanations (SHAP) framework was used [49, 50]. It provides the SHAP value for each feature for all samples and explains how much an increase in each feature value can affect the predicted probability for each clinical subgroup (non-anomaly carriers, ATL, HAM/TSP, and anomaly carriers). A higher SHAP value indicates a greater impact on the classification of a sample into a specific subgroup, while a lower SHAP value corresponds to a smaller impact. In this section, four classifiers (RF, ETC, XGB, and SVM) were explored for their performance in terms of PRAUC using nested cross-validation and were calculated for 1000 different random seeds (i.e., different values for parameter random_state). Different random seeds are considered in this study because we wanted to extract the SHAP value which is consistent whenever the randomized manipulation during the learning process is different. This allows us to evaluate the results with a high degree of confidence. For each random seed, hyperparameters were optimized on all data without cross-validation by GridSearch and used for calculating SHAP value. The absolute median of the SHAP value from all samples was collected for 1000 random seeds, and then the absolute median value and its standard deviation were calculated for visualization. Specifically, KernelSHAP was applied for all classifiers in a SHAP python package (Version 0.45.1) [50].

Data Availability

The dataset used for this study is not publicly available due to patient privacy concerns but may be made available from the corresponding author on request. All codes and files associated with this study are deposited and publicly available in the GitHub repository: https://github.com/petadimensionlab/HTLV1-machine-learning

Acknowledgment

This work was supported by Japan Agency for Medical Research and Development, Grant/Award Number 21fk0108088h0003 and 22gm1710004h0001, Japan Science and Technology Agency (JST) Grant Number JPMJCR23J4, and JST Moonshot R&D Grant Number JPMJMS2021, JPMJMS2024-9 (to S.N.).

References

1. Poiesz BJ, Ruscetti FW, Gazdar AF, Bunn PA, Minna JD, Gallo RC. Detection and isolation of type C retrovirus particles from fresh and cultured lymphocytes of a patient with cutaneous T-cell lymphoma. Proc Natl Acad Sci U S A. 1980;77(12):7415-7419. doi:10.1073/pnas.77.12.7415
2. Nagasaka M, Yamagishi M, Yagishita N, et al. Mortality and risk of progression to adult T cell leukemia/lymphoma in HTLV-1-associated myelopathy/tropical spastic

paraparesis. Proc Natl Acad Sci U S A. 2020;117(21):11685-11691. doi:10.1073/pnas.1920346117
3. Saito M. Neuroimmunological aspects of human T cell leukemia virus type 1-associated myelopathy/tropical spastic paraparesis. J Neurovirol. (2014) 20:164–74. doi: 10.1007/s13365-013-0192-8
4. Iwanaga M. Epidemiology of HTLV-1 Infection and ATL in Japan: An Update. Front Microbiol (2020) 11:1124. doi: 10.3389/fmicb.2020.01124
5. Martin, F., Fedina, A., Youshya, S., & Taylor, G. P. (2010). A 15-year prospective longitudinal study of disease progression in patients with HTLV-1 associated myelopathy in the UK. Journal of Neurology, Neurosurgery & Psychiatry, 81(12), 1336-1340.
6. Cook, Lucy B., et al. "HTLV-1: persistence and pathogenesis." Virology 435.1 (2013): 131-140.
7. Mortreux, F., Gabet, AS. & Wattel, E. Molecular and cellular aspects of HTLV-1 associated leukemogenesis in vivo. Leukemia 17, 26–38 (2003). https://doi.org/10.1038/sj.leu.2402777
8. Gonçalves, Denise Utsch, et al. "Epidemiology, treatment, and prevention of human T-cell leukemia virus type 1-associated diseases." Clinical microbiology reviews 23.3 (2010): 577-589.
9. Yamano, Yoshihisa, and Tomoo Sato. "Clinical pathophysiology of human T-lymphotropic virus-type 1-associated myelopathy/tropical spastic paraparesis." Frontiers in microbiology 3 (2012): 389.
10. Enose-Akahata Y, Abrams A, Johnson KR, Maloney EM, Jacobson S. Quantitative differences in HTLV-I antibody responses: classification and relative risk assessment for asymptomatic carriers and ATL and HAM/TSP patients from Jamaica. Blood. 2012;119(12):2829-2836. doi:10.1182/blood-2011-11-390807
11. Zhang, Ll., Wei, Jy., Wang, L. et al. Human T-cell lymphotropic virus type 1 and its oncogenesis. Acta Pharmacol Sin 38, 1093–1103 (2017). https://doi.org/10.1038/aps.2017.17
12. Brites C, Grassi MF, Quaresma JAS, Ishak R, Vallinoto ACR. Pathogenesis of HTLV-1 infection and progression biomarkers: An overview. Braz J Infect Dis. 2021;25(3):101594. doi:10.1016/j.bjid.2021.101594
13. Eusebio-Ponce E, Anguita E, Paulino-Ramirez R, Candel FJ. HTLV-1 infection: An emerging risk. Pathogenesis, epidemiology, diagnosis and associated diseases. Rev Esp Quimioter. 2019;32(6):485-496.
14. Iwanaga M, Watanabe T, Utsunomiya A, et al. Human T-cell leukemia virus type I (HTLV-1) proviral load and disease progression in asymptomatic HTLV-1 carriers: a nationwide prospective study in Japan. Blood. 2010;116(8):1211-1219. doi:10.1182/blood-2009-12-257410
15. Matsuzaki, T., Nakagawa, M., Nagai, M., Usuku, K., Higuchi, I., Arimura, K., et al. (2001). HTLV-1 proviral load correlates with progression of motor disability in HAM/TSP: analysis of 239 HAM/TSP patients including 64 patients followed up for 10 years. J. Neurovirol. 7, 228–234. doi: 10.1080/13550280152403272

16. Kwaan, Nicholas, et al. "Long-Term Variations in Human T Lymphotropic Virus (HTLV)–I and HTLV-II Proviral Loads and Association with Clinical Data." The Journal of infectious diseases 194.11 (2006): 1557-1564.
17. Okayama A, Stuver S, Matsuoka M, et al. Role of HTLV-1 proviral DNA load and clonality in the development of adult T-cell leukemia/lymphoma in asymptomatic carriers., Int J Cancer, 2004, vol. 110 4(pg. 621-625)
18. Harding D, Rosadas C, Tsoti SM, et al. Refining the risk of HTLV-1-associated myelopathy in people living with HTLV-1: identification of a HAM-like phenotype in a proportion of asymptomatic carriers. J Neurovirol. 2022;28(4-6):473-482.
19. Burbelo PD, Meoli E, Leahy HP, et al. Anti-HTLV antibody profiling reveals an antibody signature for HTLV-1-associated myelopathy/tropical spastic paraparesis (HAM/TSP). Retrovirology. 2008;5:96.
20. Akimoto M, Kozako T, Sawada T, et al. Anti-HTLV-1 tax antibody and tax-specific cytotoxic T lymphocyte are associated with a reduction in HTLV-1 proviral load in asymptomatic carriers. J Med Virol. 2007;79(7):977-986. doi:10.1002/jmv.20807
21. Yamada A, Yasunaga JI, Liang L, Zhang W, Sunagawa J, Nakaoka S, Iwami S, Kogure Y, Ito Y, Kataoka K, Nakagawa M, Iwanaga M, Utsunomiya A, Koh KR, Watanabe T, Nosaka K, Matsuoka M. Cancer Sci. 2024 Jan;115(1):310-320.
22. Enose-Akahata Y, Abrams A, Massoud R, et al. Humoral immune response to HTLV-1 basic leucine zipper factor (HBZ) in HTLV-1-infected individuals. Retrovirology. 2013;10:19. Published 2013 Feb 13. doi:10.1186/1742-4690-10-19
23. Esteva, A., Chou, K., Yeung, S. et al. Deep learning-enabled medical computer vision. npj Digit. Med. 4, 5 (2021). https://doi.org/10.1038/s41746-020-00376-2
24. Bock, C., Walter, J.E., Rieck, B. et al. Enhancing the diagnosis of functionally relevant coronary artery disease with machine learning. Nat Commun 15, 5034 (2024). https://doi.org/10.1038/s41467-024-49390-y
25. Dietterich, T. G. in Joint IAPR International Workshops on Statistical Techniques in Pattern Recognition (SPR) and Structural and Syntactic Pattern Recognition (SSPR) vol. 2396 15–30 (Springer, 2002).
26. Krumholz, H. M. Big data and new knowledge in medicine: the thinking, training, and tools needed for a learning health system. Health Aff. 33, 1163–1170 (2014).
27. Tomašev, N. et al. A clinically applicable approach to continuous prediction of future acute kidney injury. Nature 572, 116–119 (2019).
28. O'Brien, R. M. (2007). A Caution Regarding Rules of Thumb for Variance Inflation Factors. *Quality & Quantity*, 41(5), 673–690.
29. Akbarin MM, Rahimi H, Hassannia T, Shoja Razavi G, Sabet F, Shirdel A. Comparison of HTLV-I Proviral Load in Adult T Cell Leukemia/Lymphoma (ATL), HTLV-I-Associated Myelopathy (HAM-TSP) and Healthy Carriers. Iran J Basic Med Sci. 2013;16(3):208-212.
30. Grassi MFR, Olavarria VN, Kruschewsky RA et al (2011) Human T cell lymphotropic virus type 1 (HTLV-1) proviral load of HTLV-associated myelopathy/tropical spastic paraparesis (HAM/TSP) patients according to new diagnostic criteria of HAM/TSP. 1274:1269–74. 10.1002/jmv

31. Igakura, T., Stinchcombe, J. C., Goon, P. K., Taylor, G. P., Weber, J. N., Griffiths, G. M. & Bangham, C. R. (2003). Spread of HTLV-I between lymphocytes by virus-induced polarization of the cytoskeleton. Science, 299(5613), 1713-1716.
32. Delamarre L, Rosenberg AR, Pique C, Pham D, Dokhélar MC. A novel human T-leukemia virus type 1 cell-to-cell transmission assay permits definition of SU glycoprotein amino acids important for infectivity. J Virol. 1997;71(1):259-266. doi:10.1128/JVI.71.1.259-266.1997
33. Derse D, Hill SA, Lloyd PA, Chung Hk, Morse BA. Examining human T-lymphotropic virus type 1 infection and replication by cell-free infection with recombinant virus vectors. J Virol. 2001;75(18):8461-8468. doi:10.1128/jvi.75.18.8461-8468.2001
34. Santana CS, Andrade FdO, da Silva GCS, Nascimento JOdS, Campos RF, Giovanetti M, Santos LA, Gois LL, Alcantara LCJ and Barreto FK (2023) "Advances in preventive vaccine development against HTLV-1 infection: A systematic review of the last 35 years." Front. Immunol. 14:1073779.
35. Nakamura M, Kuroki M, Kira J, et al. Elevated antibodies to synthetic peptides of HTLV-1 envelope transmembrane glycoproteins in patients with HAM/TSP. J Neuroimmunol. 1991;35(1-3):167–177.
36. Sagara Y, Inoue Y, Tsujimura M, Kojima E, Shiraki H, Kashiwagi S. Novel biomarker of HTLV-1-associated disease: specific appearance of antibody recognizing the receptor-binding site on HTLV-1 envelope protein. Cancer Sci. 2004;95(10):835–839.
37. Enose-Akahata Y, Vellucci A, Jacobson S. Role of HTLV-1 Tax and HBZ in the Pathogenesis of HAM/TSP. Front Microbiol. 2017;8:2563. Published 2017 Dec 21. doi:10.3389/fmicb.2017.02563
38. Le Blanc IBlot V, Bouchaert I, Salamero J, Goud B, Rosenberg AR, Dokhélar M.2002.Intracellular Distribution of Human T-Cell Leukemia Virus Type 1 Gag Proteins Is Independent of Interaction with Intracellular Membranes. J Virol76:.https://doi.org/10.1128/jvi.76.2.905-911.2002
39. Pedregosa, F., Varoquaux, G., Gramfort, A., Michel, V., Thirion, B., Grisel, O., Blondel, M. (2011). Scikit-learn: Machine learning in Python. Journal of Machine Learning Research, 12(Oct), 2825-2830. https://scikit-learn.org/
40. Charles R. M. Bangham; HTLV-1 persistence and the oncogenesis of adult T-cell leukemia/lymphoma. Blood 2023; 141 (19): 2299–2306.
41. Yamauchi, Junji, et al. "An update on human T-cell leukemia virus type I (HTLV-1)-associated myelopathy/tropical spastic paraparesis (HAM/TSP) focusing on clinical and laboratory biomarkers." Pharmacology & Therapeutics 218 (2021): 107669.
42. Penova, M., Kawaguchi, S., Yasunaga, J. I., Kawaguchi, T., Sato, T., Takahashi, M., ... & Matsuda, F. (2021). Genome wide association study of HTLV-1–associated myelopathy/tropical spastic paraparesis in the Japanese population. Proceedings of the National Academy of Sciences, 118(11), e2004199118.
43. Liu, F. T., Ting, K. M. & Zhou, Z. Isolation Forest. *8th IEEE Int. Conf. Data Min*. https://ieeexplore.ieee.org/document/4781136/ (2008).
44. Chandola, V., Banerjee, A., & Kumar, V. (2009). Anomaly detection: A survey. ACM Computing Surveys (CSUR), 41(3), 1-58.

45. Enose-Akahata, Y., Jacobson, S. Immunovirological markers in HTLV-1-associated myelopathy/tropical spastic paraparesis (HAM/TSP). *Retrovirology* 16, 35 (2019).
46. Saito T, Rehmsmeier M (2015) The Precision-Recall Plot Is More Informative than the ROC Plot When Evaluating Binary Classifiers on Imbalanced Datasets. PLOS ONE 10(3): e0118432.
47. Eric Jones, Travis Oliphant, Pearu Peterson, et al. (2001). SciPy: Open source scientific computing tools for Python. https://scipy.org/
48. Virtanen P., Gommers R, Oliphant TE, Haberland M, Reddy T, Cournapeau D, et al. SciPy 1.0: Fundamental Algorithms for Scientific Computing in Python. Nature Methods. 2020;17:261–272. Pmid:32015543
49. Shapley, L. S. 17. A value for n-person games. In Contributions To The Theory of Games (AM-28), Volume II (eds. Kuhn, H. W., Tucker, A. W.) 307–318.
50. Lundberg, S. M. & Lee, S.-I. A unified approach to interpreting model predictions.

Supplementary Information

Supplementary Tables

Features	**VIF Score** (all features)
PVL	1.145
Tax	1.654
Env	3.042
Gag p15	1.314
Gag p19	7.481
Gag p24	6.141

Supplementary Table S1A: This table represents the feature values with the respective VIF scores. Gag p19 showed the highest VIF score of 7.480 for Gag p19, indicative of substantial multicollinearity. To mitigate this, Gag p19 was removed from the dataset.

Features	**VIF Score** (Gag p19 removed)
PVL	1.110
Tax	1.631
Env	2.462
Gag p15	1.293
Gag p24	2.794

Supplementary Table S1B: This table shows the reduction in VIF scores across all features after removing Gag p19. Recalculations of the VIF scores for the remaining features demonstrated a significant reduction in multicollinearity with all features displaying VIF-score < 3, suggesting that the remaining set of features PVL, Tax, Env, Gag p15 and p24 exhibits minimal multicollinearity and suitable for further analysis [O'Brien, R. M.].

Features	Spearman's rank correlation coefficient (r) among the feature values and the anomaly scores of the anomaly carrier data	p-value
Gag p15	-0.67	0.003*
Gag p24	-0.55	0.022*
Env	-0.52	0.032*
Tax	-0.27	0.299
PVL	0.1	0.701

Supplementary Table S2: Spearman's rank correlation coefficients (r) illustrate the relationships between the feature values of the anomaly carriers (n=17) and their corresponding anomaly scores as determined by the Isolation forest anomaly detection model. * indicates a statistically significant correlation (p-value <0.05).

Classifier names	Overall Mean PRAUC (One-vs-Rest multiclass classification)
Random Forest (RF)	0.841
XGBoost (XGB)	0.819
Extra Tree Classifier (ETC)	0.839
Support Vector Machine (SVM)	0.811

Supplementary Table S3: Overall Mean PRAUC of the classifiers used in our study.

Feature names	Spearman's rank correlation coefficient (r)	p-value
Gag p15	0.649	0.004*
Gag p24	0.618	0.008
Env	0.444	0.073
Tax	0.108	0.679
PVL	0.036	0.888

Supplementary Table S4: Spearman's rank correlation coefficients (r) between the feature values of the anomaly carriers (n=17) and their predicted probability of belonging to HAM/TSP, as determined by the random forest classifier model. All the feature values except PVL showed a stronger positive correlation with the predicted probability of HAM/TSP. However, none of these were statistically significant except Gag p15. * indicates a statistically significant correlation (p-value <0.05).

Carrier ID	PVL (%)	Tax	Env	Gag p15	Gag p24	Anomaly Score
indiv0027	35.1	46360.6	8036.57	133435.5	9186793	-0.227
indiv0035	46.3	6257.36	3380.86	1392	557465.7	-0.107
indiv0069	2.73	5475.765	6935.648	334938.483	10298208.9	-0.206
indiv0086	2.8	85900.225	4353.48	9175.32	7825533.16	-0.135
indiv0125	3.52	24760.56	9624	143221.032	10627154.2	-0.143
indiv0131	1.89	9997.35	10307.304	156990.407	8509020.98	-0.110
indiv0133	1.54	6710.417	2773.046	62421.852	7597349.42	-0.051
indiv0169	2.79	73261.68	10899.912	156270.114	5645401.27	-0.160
indiv0189	0.36	112722.516	2923.854	365.62	14694.135	-0.113
indiv0217	7.09	40165.452	8748.922	232614.22	5608868.82	-0.136
indiv0221	9.79	5629.212	14189.266	89869.177	5905812.24	-0.133
indiv0227	7.16	65582	14497.938	264498.926	7607445.6	-0.215
indiv0240	7.49	12044.324	9279.452	127028.479	8400371.16	-0.087
indiv0245	23.47	1863.456	3303.802	44529.681	1584100.75	-0.051
indiv0249	11.55	76016.766	3491.858	8507.275	665555.814	-0.072
indiv0254	5.07	28942.788	5466.446	335210.855	10180285.4	-0.204
indiv0265	19.76	29540.5446	7478.61089	65475.1918	4953871.65	-0.107

Supplementary Table S5: This table represents the HTLV-1 Pro-viral load (PVL) and the antibody titer profile of the anomaly carrier samples with their respective anomaly scores obtained from the Isolation forest anomaly detection model. The sklearn implementation of the decision function of Isolation Forest yields anomaly scores, where negative scores indicate potential anomalies and positive scores indicate non-anomalies.

Pairwise comparisons	**PVL**	**Tax**	**Env**	**Gag p15**	**Gag p19**	**Gag p24**
Carrier vs Anomaly carrier	Significant P= 0.0197	Significant P= 0.0000	Significant P=0.0000	Significant P=0.0000	Significant P=0.0000	Significant P=0.0000
HAM vs Anomaly carrier	Not significant P= 1.0000	Not significant P= 1.0000	Significant P=0.0048	Not significant P= 0.3395	Not significant P= 0.6504	Not significant P= 0.8887
ATL vs Anomaly carrier	Significant P= 0.0190	Significant P=0.0001	Significant P=0.0000	Significant P=0.0000	Significant P=0.0446	Significant P=0.0137
Carrier vs HAM	Significant P= 0.0000	Significant P=0.0000	Not significant P= 0.3102	Significant P=0.0000	Significant P=0.0000	Significant P=0.0000
Carrier vs ATL	Significant P= 0.0000	Not Significant p= 1.0000	Not significant P= 1.0000	Not significant P= 1.0000	Significant P=0.0054	Significant P=0.0095
HAM vs ATL	Significant P= 0.0000	Significant P=0.0000	Not significant P= 0.1995	Significant P=0.0000	Not significant P= 0.6865	Not significant P= 0.1148

Supplementary Table S6: Dunn's post-hoc analysis followed by the Kruskal-Wallis test. This table demonstrates statistical differences between pairwise comparisons of the sample groups.

Features	Spearman's rank correlation coefficient(r) with PVL of Carrier	p-value
Env	0.488	3.277221599473032e-17*
Gag p24	0.390	4.718707358480701e-11*
Gag p15	0.310	2.724230441420774e-07*
Tax	0.183	0.002723751725992901*

Supplementary Table S7: Spearman's rank correlation analysis between PVL and other features among the Carrier population (n=264). * indicates a statistically significant correlation (p-value <0.05).

Features	Spearman's rank correlation coefficient(r) with PVL of HAM/TSP	p-value
Gag p15	0.311	0.019*
Gag p24	0.216	0.108
Env	0.192	0.154

Tax	-0.063	0.642

Supplementary Table S8: Spearman's rank correlation analysis between PVL and other features among the HAM population (n=56). * indicates a statistically significant correlation (p-value <0.05).

Features	Spearman's rank correlation coefficient(r) with PVL of ATL	p-value
Env	-0.631	1.16443058497141 9e-06*
Gag p15	-0.257	0.073
Tax	-0.162	0.264
Gag p24	-0.004	0.977

Supplementary Table S9: Spearman's rank correlation analysis between PVL and other features among the ATL population (n=49). * indicates a statistically significant correlation (p-value <0.05).

Supplementary Figures

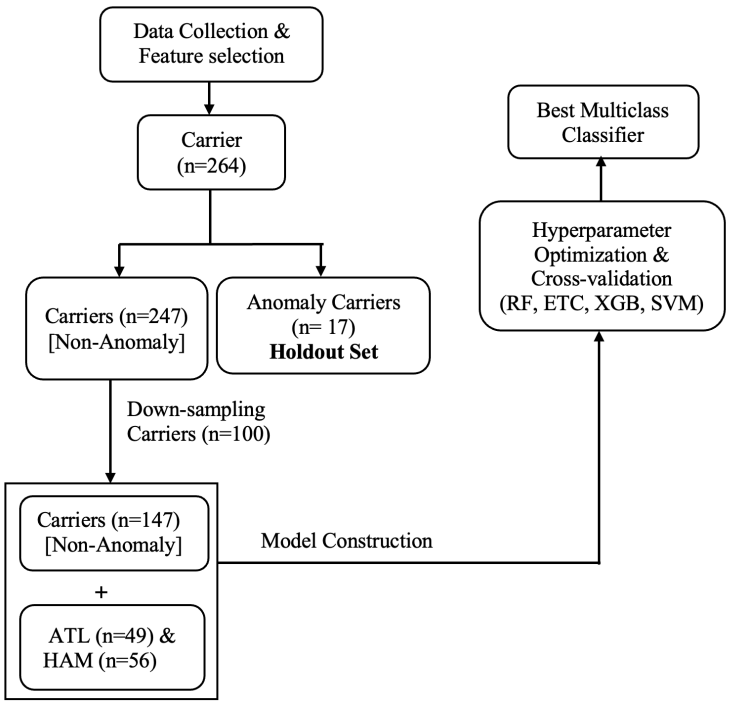

Supplementary Figure S1: Workflow chart

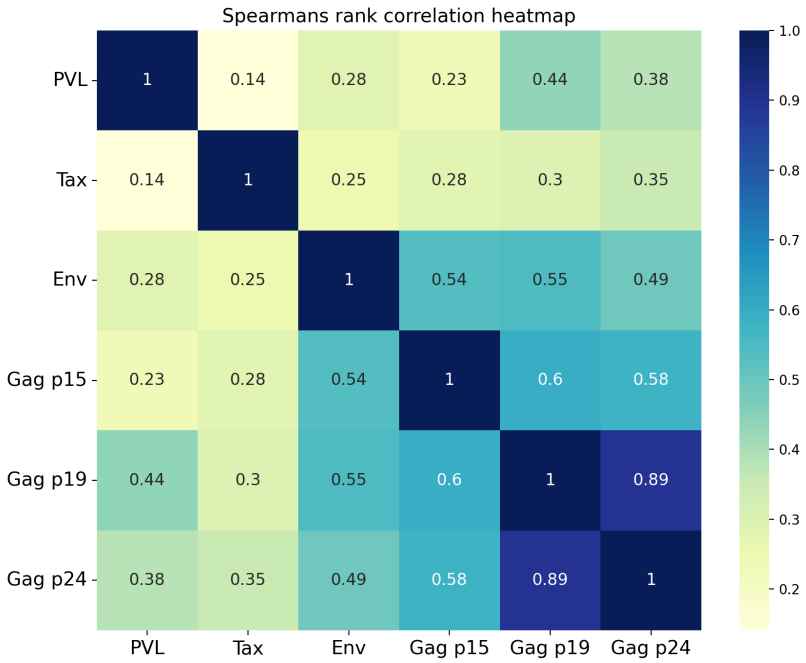

Supplementary Figure S2: Spearman rank correlation heatmap among the feature values of all samples.

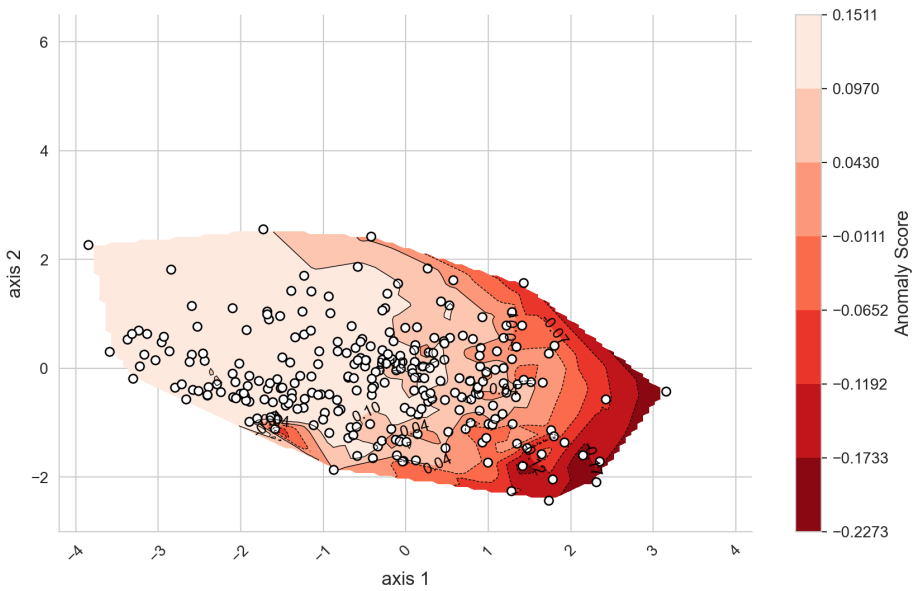

Supplementary Figure S3: The contour plot provides a visual representation of the anomaly score distribution for the carrier-only data. Data points are higher in the lighter red areas, suggesting that most carriers have similar characteristics or behaviors, indicating they are less anomalous. In contrast, the points in regions with higher anomaly scores (darker shades) are more likely to be anomalies or outliers. The spread along these axes indicates how the data

varies across these two dimensions. The color bar on the right provides a scale for the anomaly scores. Higher anomaly scores (darker shades) indicate a higher likelihood of being an anomaly.

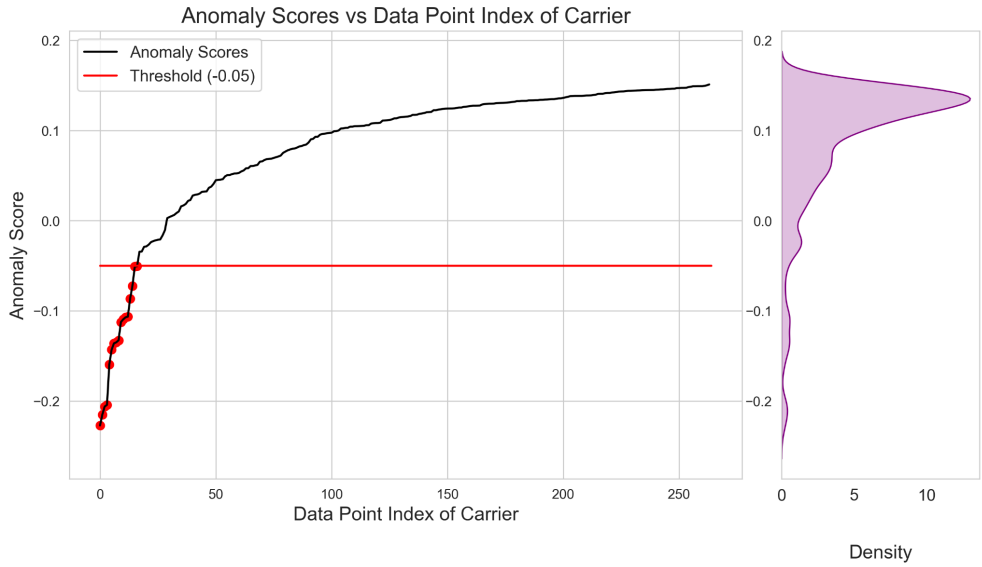

Supplementary Figure S4: This figure shows the Isolation forest anomaly scores plotted against the carrier data point index (n=264) with a threshold of -0.05. The plot demonstrates that most data points have anomaly scores above the threshold (-0.05). Data points below the threshold were considered anomaly samples in our study and thus highlighted in red circles. The vertical figure on the right demonstrates the KDE distribution plot of the anomaly scores among the carrier population.

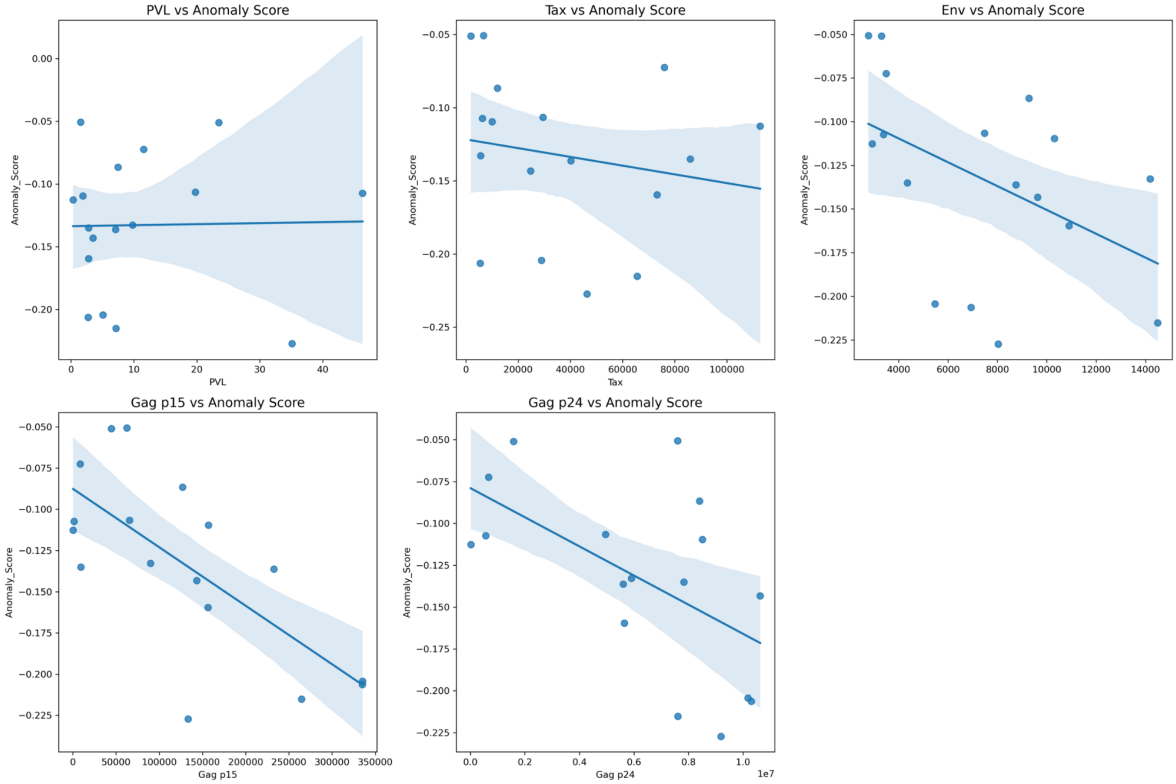

Supplementary Figure S5: All features except PVL show a negative correlation with their respective feature values, indicating that as the feature value increases, the anomaly score tends to decrease (in sklearn implementation of Isolation forest, negative anomaly scores indicate anomalies). The strength of the negative correlation varies among the features, with Gag p15 showing the most substantial negative correlations compared to other features. The plots collectively suggest that higher values in the features Tax, Env, Gag p15, and Gag p24 are generally associated with lower anomaly scores. The shaded area indicates a 95% confidence interval.

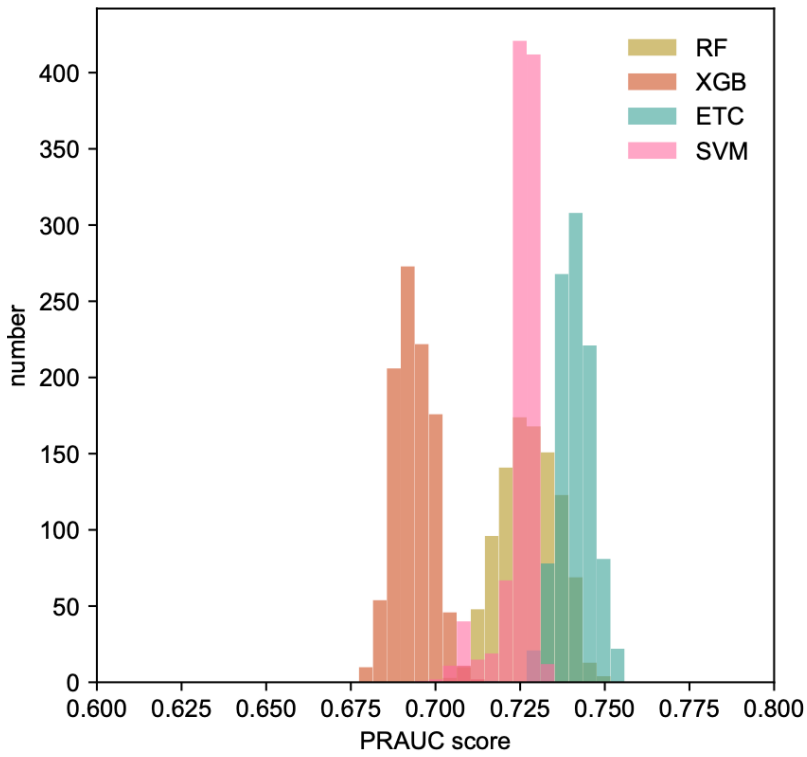

Supplementary Figure S6: Histogram of performance for each classifier in terms of PRAUC. Each distribution was made from 1000 iterations of different random seeds (random_state parameter). In this study, 1000 patterns of random seeds are considered to evaluate the performance with a high degree of confidence. These results obtained from different random seeds then turn out to be reliable whenever the randomized manipulation during the learning process is different.

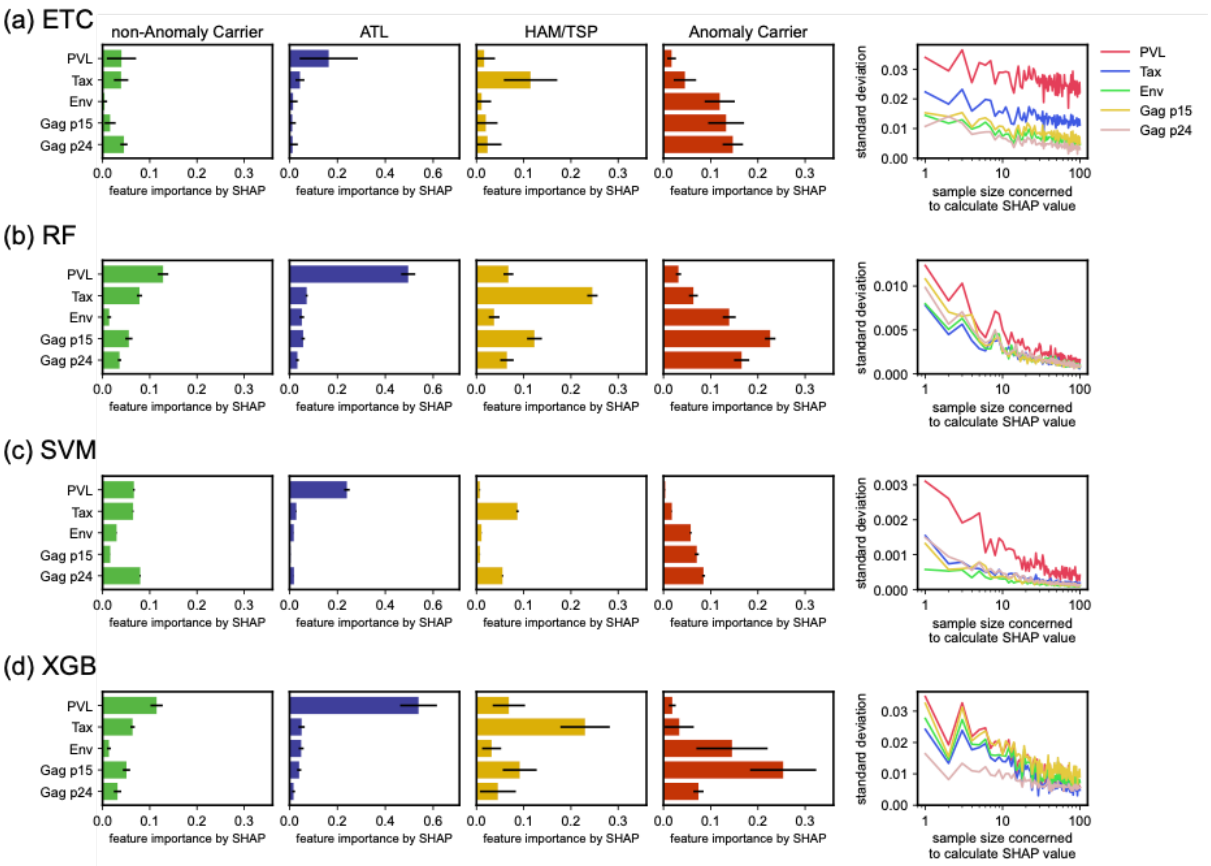

Supplementary Figure S7: SHAP bar plot for each subgroup (non-anomaly carrier, ATL, HAM/TSP, and anomaly carrier) for each classifier (ETC, RF, SVM, and XGB) (left four panels). Each SHAP bar is a median value from 1000 iterations of different random seeds and the black line represents a standard deviation. The most right panel shows the standard deviation calculated from ten sets of different median SHAP values for each feature. In each set, a random seed is randomly picked from 1 to 100 and the median value is chosen (this is the x-axis). The figure showed that 100 iterations can converge to settle near zero; thus the SHAP bar plot was calculated using 1000 iterations (10 times higher). While the best-performing classifier was ETC [Supplementary Figure S6], the PRAUC scores of the four classifiers were comparable. Hence, we stuck to the idea that only consistent trends in SHAP values among all classifiers were considered reliable (SHAP values were consistent among all classifiers except for Gag p24).